Chaotic dynamics of a convection roll in a highly confined, vertical, differentially heated fluid layer

Zhenlan GAO[1,2,3], Bérengère Podvin[1], Anne Sergent[1,2] & Shihe Xin[4]

[1] CNRS, LIMSI, UPR3251, BP 133, 91403, Orsay Cedex, France
[2] Universite Pierre et Marie Curie - Paris 06, 4 Place Jussieu, 75252 Paris, Cedex 05, France
[3] Arts et Métiers ParisTech, 2 Boulevard du Ronceray, 49035 Angers Cedex 01, France
[4] CETHIL, INSA de Lyon, 69621 Villeurbanne Cedex, France
gao@limsi.fr

Résumé. Le comportement chaotique d'un rouleau de convection dans une couche de fluide verticale, confinée, et differentiellement chauffée est présenté. Le chaos temporel est atteint par une séquence de doublements de période. Au nombre de Rayleigh plus élevé, l'intermittence induite par la crise a été observée. Un modèle à trois équations est proposé. Il peut répresenter correctement le dynamique du rouleau de convection.
Abstract. The chaotic behavior of a single convection roll in a highly confined, vertical, differentially heated fluid layer is studied in the present work. The chaos occurs through a sequence of period-doubling bifurcation. At higher Rayleigh number, a crisis-induced intermittency is observed. A three-equation model is proposed and successfully captures the dynamics of the convection roll.

1 Introduction

Natural convection between two vertical differentially heated plates is considered as a classic prototype for many industrial applications, for example, the doubled-panel window or the plate heat exchangers. Depending on the aims of applications, the transition to turbulence is intented to be promoted or delayed. In the present study, we consider the instabilities onset and chaotic behavior of the flow, when the Rayleigh number Ra is increased. The flow is characterised by cat's eye-like convection rolls when Ra is above the critical Rayleigh number $\mathrm{Ra_c} = 5708$. At higher Ra, these convection rolls are found to be connected by oblique vorticity braids in the case of a transversely confined domain [1,2]. In this work we focus on the dynamics of a single convection roll by considering a small periodic domain, using direct numerical simulation (DNS) [3]. In the spirit of [9], we derive a low-order model to capture the main dynamics of the flow.

2 Physical model and numerical methods

The flow of air between two infinite vertical plates maintained at different temperatures is considered as in Figure 1 (a). The distance between the plates is D, and the periodic dimensions of the plates are L_z and L_y respectively. The temperature difference between the two plates is ΔT. The direction x is normal to the plates, the transverse direction is y, and the gravity g is opposite to the vertical direction z. The fluid properties of air, such as kinetic viscosity ν, thermal diffusivity κ, thermal expansion coefficient β, are constant. Four nondimensional parameters characterizing the flow are the Prandtl number $\mathrm{Pr} = \frac{\nu}{\kappa}$, the Rayleigh number based on the width of the gap between the two plates $\mathrm{Ra} = \frac{g\beta\Delta T D^3}{\nu\kappa}$, and the transverse and vertical aspect ratio $A_y = L_y/D$ and $A_z = L_z/D$, respectively. Only the Rayleigh number is varied in the present study. The Prandtl number of air is fixed to 0.71. The transverse aspect ratio is set to be $A_y = 1$, the vertical aspect ratio is set to $A_z = 2.5$, which corresponds to the critical wavelength $\lambda_{zc} = 2.513$ obtained by the stability analysis [1].

2.1 Equations of motion

The flow is governed by the Navier-Stokes equations within the Boussinesq approximation. Here t denotes time, $\overrightarrow{u} = (u, v, w)$ is the velocity vector, p is the pressure, θ is the temperature. The nondimensionalized equations are:

$$\nabla \cdot \overrightarrow{u} = 0 \tag{1}$$

$$\frac{\partial \overrightarrow{u}}{\partial t} + \overrightarrow{u} \cdot \nabla \overrightarrow{u} = -\nabla p + \frac{\mathrm{Pr}}{\sqrt{\mathrm{Ra}}} \Delta \overrightarrow{u} + \mathrm{Pr}\theta \overrightarrow{z} \tag{2}$$

$$= \frac{1}{\sqrt{\mathrm{Ra}}} \Delta \theta \tag{3}$$

with Dirichlet boundary conditions at the plates

$$\overrightarrow{u}(0, y, z, t) = \overrightarrow{u}(1, y, z, t) = 0, \quad \theta(0, y, z, t) = 0.5, \quad \theta(1, y, z, t) = -0.5 \tag{4}$$

and periodic conditions in the y and z directions.

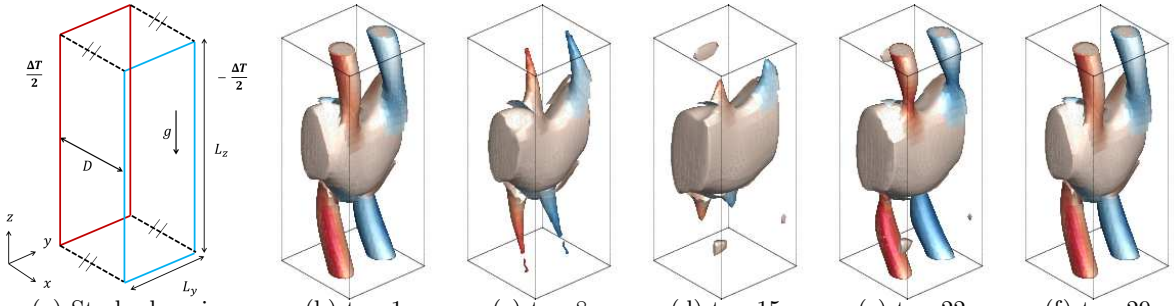

(a) Study domain (b) t = 1 (c) t = 8 (d) t = 15 (e) t = 22 (f) t = 29

Figure 1. (a) Study domain; (b)-(f): Q-criterion visualization of flow structure at selected times spanning one oscillation period at $Ra = 11500$, $Q = 0.1$ colored with vorticity Ω_x.

2.2 Numerical methods

A spectral code [3] developped at LIMSI is used to carry out the simulations. The spatial domain is discretized by the Chebyshev-Fourier collocation method. The projection-correction method is used to enforce the incompressibility of the flow. The equations are integrated in time with a second-order mixed explicit-implicit scheme. A Chebyshev discretization with 40 modes is applied in the direction x, while the Fourier discretization is used in the transverse and vertical directions. 30 Fourier modes are used in the transverse direction y for $A_y = 1$, while 60 Fourier modes are used in the vertical direction z for $A_z = 2.5$. Convergence of the spatial discretization has been established [1]. We run our simulations by following a branch of stable solutions. An instantaneous flow realization in the periodic regime at Ra = 11300 is taken as the initial condition for the first run. For each following run, the Rayleigh number is increased by an small increment ΔRa of 2. At each Ra, the data is sampled when the asymptotic regime has been reached, i.e after long time numerical integrations (about 10^4 nondimensional time units). A solution in this asymptotic regime is then used as the initial condition for the simulation at the next higher Ra.

3 DNS results

3.1 Periodic regime

As reported in [1], the flow becomes 2D steady then 3D steady through two supercritical pitchfork bifurcations at Ra = 5708 and Ra = 9980. The flow structure consists of a primary roll deformed in its transverse direction, with two counter-rotating braids of oblique vorticity originating from the roll [1]. Then via a Hopf bifurcation at Ra = 11270, the flow becomes time-dependent. The roll and braids grow and shrink alternatively and periodically as shown in 1 (b)-(f), where the periodic exchanges of energy and enstrophy between the primary roll and braids take place. The time period of the oscillation T_{osc}^{DNS} is about 28 convective units.

Spatial 2D Fourier analysis can provide a useful description of the flow. For example the vertical velocity can be expressed as $w(x, y, z, t) = \sum_{lk} \hat{w}_{lk}(x, t) e^{2i\pi(\frac{ly}{A_y} + \frac{kz}{A_z})}$, where $i = \sqrt{-1}$. The first Fourier modes $\hat{w}_{lk}$ of the vertical velocity on the plane at $x = 0.0381$ are represented in Figure 2 for l, k equal to 0 or 1. We checked that these results did not depend on the distance of the plane to the wall. It

confirms that the energy is concentrated in the mean mode $\hat{w}_{00}$, then in the first Fourier mode in each direction $\hat{w}_{01}$ and $\hat{w}_{10}$. All other modes represent less than 8% energy of mode $\hat{w}_{10}$. This suggests that the dynamics is restricted to a limited number of degrees of freedom and could be approximated with a low order model (see section 4).

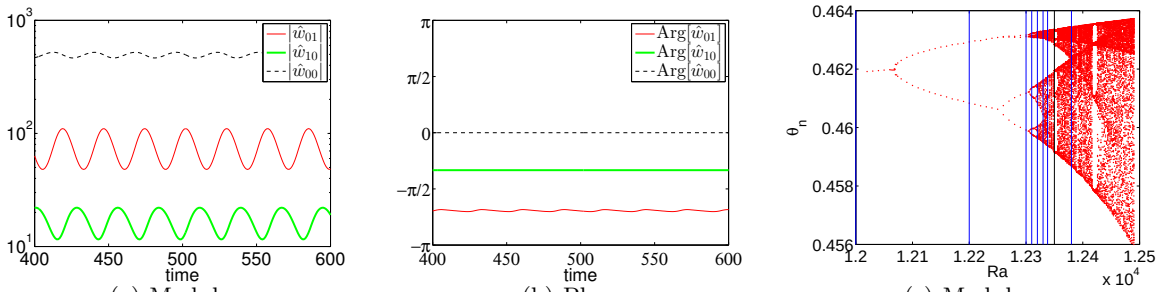

(a) Modulus (b) Phase (c) Modulus

Figure 2. (a)-(b) Temporal evolutions of Fourier modes $\hat{w}_{lk}$ obtained by the Fourier transform of the vertical velocity w distribution on an arbitrarily chosen vertical plane at $x = 0.0381$, Ra $= 11500$. (c) Bifurcation diagram obtained by using the local maxima θ_n of the temperature timeseries at the point (0.038 0.097 0.983).

3.2 Period-doubling cascade

As the Rayleigh number increases, a sequence of period-doubling bifurcations is observed, which leads the flow to a temporally chaotic regime [1]. A bifurcation diagram of Figure 2 (c) is constructed from local maxima θ_n of the temperature timeseries at the point (0.038 0.097 0.983). With a linear extrapolation, we estimated the local critical Rayleigh numbers for each period-doubling bifurcation, from which we calculated the Feigenbaum constants (Table 3.2). Some agreement with the theoretical value $\delta = 4.66920161....$ is observed [4]. Using the theoretical Feigenbaum number, the chaotic regime is estimated to be reached around Ra ~ 12320. For higher Rayleigh numbers, the chaos continues to develop as shown in the bifurcation diagram (Figure 2 (c)). Several periodic windows are also observed. For example, a large '*period-6* windows' is observed at Ra $= 12350$ in Figure 2 (c). We used the computation technique proposed by Benettin *et al.* [5] to calculate the largest Lyapunov exponent. As shown in Figure 3 (a), the largest Lyapunov exponent is found to be positive for Ra ≥ 12360, which suggests that temporal chaos has been reached. The flow still follows the basic oscillation displayed in the periodic regime, but the maximum roll and braid amplitudes vary from one cycle to the other, as is evidenced in Figure 3 (b)-(d).

Bifurcations $2^i \to 2^{i+1}$	Local critical $\mathrm{Ra}_{2^i \to 2^{i+1}}$	Estimated Feigenbaum constant $\tilde{\delta}$
0-1	11270	
1-2	12068.09	
2-4	12258.42	4.193
4-8	12305.76	4.020
8-16	12316.72	4.321

3.3 Crisis-induced intermittency

The bifurcation diagram for the range Ra $\in [12400, 12600]$ is represented in Figure 3 (e). At Ra $= 12546$, a new set of local maxima abruptly appears on the top-right corner. This is the sign of another type of crisis [6]. Figure 4 (a) shows that the phase of the first Fourier mode $\hat{w}_{01}$ for Ra $= 12600$ intermittently experiences a shift of π. The time between phase switches appears to be random, but decreases with the Rayleigh number. A description of the flow structure is given by streamlines plots in Figure 4 (b) (c): the roll randomly switches between two vertical positions separated by a distance equal to half the wavelength of the coherent structure. The switch of flow structures suggests the existence of a heteroclinic connection between two chaotic attractors, which are located on the $O(2) \times O(2)$ invariant torus of chaotic solutions. Structurally stable heteroclinic connections between fixed points or periodic solutions have been shown to exist in the systems with $O(2)$ symmetry [7,8]. Such connections are typically associated with a $1:2$ or $0:1:2$ resonance. It is not clear if such resonances are present here. Moreover, we are not aware of

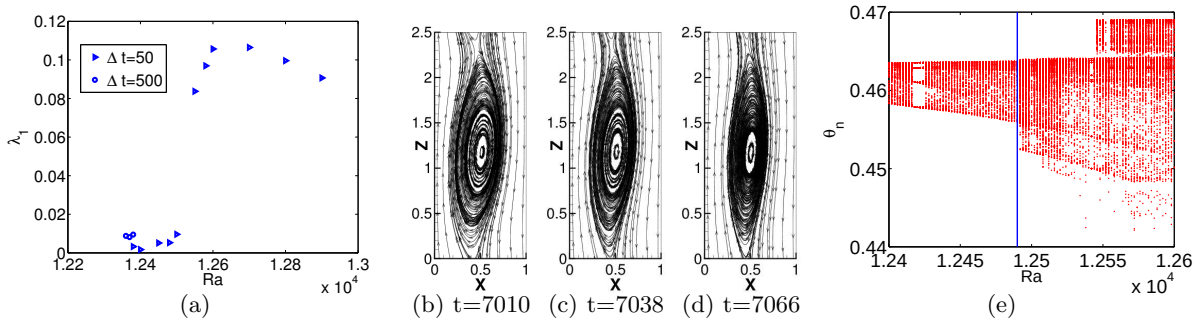

Figure 3. (a) The largest Lyapunov exponent λ_1 at different Rayleigh numbers; (b)-(d) Flow streamlines at three instants separated by a basic oscillation period $T_{osc}^{DNS} = 28$ at Ra = 12380 on the vertical planes $y = 0.5$; (e) Bifurcation diagram obtained by using the local peaks θ_n of the timeseries at the point (0.038 0.097 0.983). Note: the vertical line in the figure corresponds the largest Rayleigh number in Figure 2 (c).

theoretical results for heteroclinic connections between two strange attractors. At Ra $= [13000, 13100]$ and $[14200, 14500]$, two periodic "windows" regimes are observed. The periodic orbits correspond to both a modulation and a shift of the roll and braids. The time scale τ characterizing the average time length during which the convection roll remains at a fixed location obeys the power law $\tau \sim (\mathrm{Ra} - \mathrm{Ra}_{ci})^{-\gamma}$ with a value of $\gamma \sim 0.78$ (see Figure 4 (d)). As pointed out in [6], for one-dimensional maps with quadratic maxima, the critical crisis exponent γ is strictly equal to $\frac{1}{2}$, while for higher-dimensional maps, γ is larger than $\frac{1}{2}$. It suggests that our system has a fractal dimension larger than 1. The largest Lyapunov exponent λ_1 in the intermittency regime (Figure 3 (a)) shows an increase by a factor of 10 between the chaotic and intermittent regimes, which corresponds to the modification of the flow associated with the roll shift.

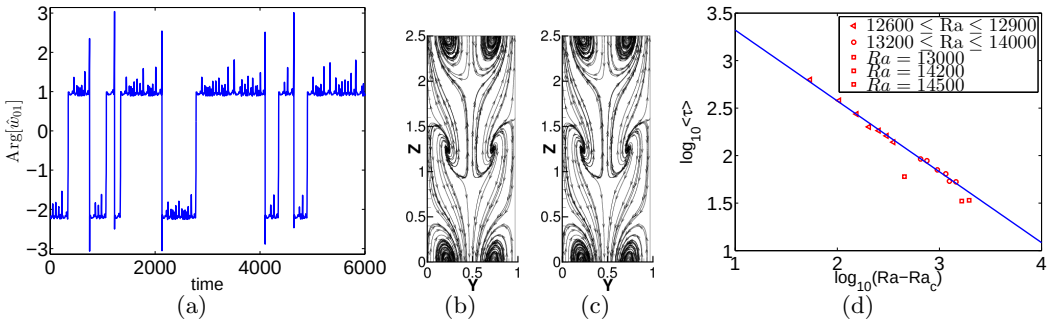

Figure 4. (a) Phase of the temporal evolution of the Fourier mode $\hat{w}_{01}$ calculated on the vertical plane $x = 0.0381$, Ra = 12600; (b)-(c) Flow streamlines at different instants on the plane $y = 0.5$; (d) $\log_{10}\langle\tau\rangle$ vs $\log_{10}(\mathrm{Ra} - \mathrm{Ra}_c)$. The slope of the straight line gives $\gamma \approx 0.78$.

4 Lower-order model

4.1 Model for the periodic regime

In the periodic regime (section 3.1), the plot of Fourier modes in Figure 2 (a) shows that the intensities of the braids and the roll fluctuate in quasi-phase opposition. The phase of the roll mode (Figure 2 (b)) is not exactly constant, which shows that the rolls lightly oscillates around a fixed position. Timeseries of the different physical variables show that all the components assoicated with a given Fourier mode oscillate in phase. Based on these observation and in the spirit of [9], we propose a three equation model to represent the flow behaviors, which reads as

$$\dot{a}_{01} = B_1(< a_{00} > -a_{00})a_{01} \tag{5}$$

$$\dot{a}_{10} = B_2(< a_{00} > -a_{00})a_{10} \tag{6}$$

$$\dot{a}_{00} = 2B_1(|a_{01}|^2 - < |a_{01}|^2 >) + 2B_2(|a_{10}|^2 - < |a_{10}|^2 >) \tag{7}$$

where $< a_{00} >$, $< |a_{01}|^2 >$, $< |a_{10}|^2 >$ are constants extracted from the DNS. The details of model derivation can be found in [10]. At Ra = 11500, using the coefficients in Table 1, the model yields a characteristics period of T about 28 convective units, in agreement with DNS. Figure shows the time series from the DNS and the model integrated from the same initial condition. The agreement between the model and the simulation is quite good for the modes $\hat{w}_{00}$ and $\hat{w}_{01}$. The less energetic mode $\hat{w}_{10}$ is not quite as well reproduced, which is likely to be an effect of truncation.

Ra	11500	12500	12800
T_{osc}^{DNS}	28	28	28
$(< \lvert\hat{w}_{01}\rvert >, \lvert\hat{w}_{01}\rvert^{min}, \lvert\hat{w}_{01}\rvert^{max})$	(88,55,127)	(88,1.7,204)	(88,0,210)
$(< \lvert\hat{w}_{11}\rvert >, \lvert\hat{w}_{10}\rvert^{min}, \lvert\hat{w}_{10}\rvert^{max})$	(48,34,61)	(48,0.93,92)	(48,0,100)
$(< \lvert\hat{w}_{00}\rvert >, \lvert\hat{w}_{00}\rvert^{min}, \lvert\hat{w}_{00}\rvert^{max})$	(818,757,882)	(837,680,1033)	(845,665,1050)
(B_1, B_2)	(1.2e-03, -0.9e-03)	(1.3e-03, -1.1e-03)	(1.2e-03,-1.1e-03)

Table 1. Statistics of the vertical velocity w in the simulation and values of the model coefficients at different Rayleigh numbers

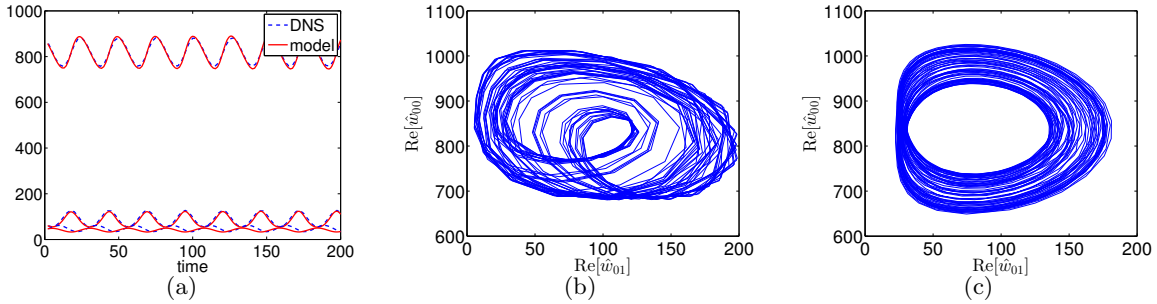

Figure 5. (a) Comparison between the model and the simulation at Ra = 11500: from top to bottom, $|\hat{w}_{00}|$, $|\hat{w}_{01}|$, $|\hat{w}_{10}|$; (b)-(c)Velocity Fourier modes on the plane $x = 0.5$ at Ra = 12500: (b) DNS, (c) model with $\beta = 0.5$, $T' = 25$

4.2 Modelling the chaotic regime

In the chaotic regime, nonlinear interaction involving modes excluded from the truncation are expected to influence the dynamics of the low-order model. The dominant mode outside the truncation is found to be pure vertical mode $\hat{w}_{02}$ We therefore simply model the influence of higher-order modes by introducing a periodic perturbation of amplitude β in the evolution equation of the vertical mode $\hat{w}_{01}$. Owing to the strong transverse confinement, we did not perturb the transverse mode $\hat{w}_{10}$, so that only equation (5) was modified as follows:

$$\dot{a}_{01} = (\mu_1 - B_1 a_{00}) a_{01} + \beta sin(2\pi t/T'). \tag{8}$$

The frequency of the perturbation $1/T'$ was chosen to be close to that of the oscillation ($T' = 25$). For the typical value $\beta = 0.5$, a modulation of the amplitudes was observed, as is evidenced by the phase portraits in Figure 5 (b) (c).

4.3 Modelling intermittency

As Ra increases, the nonlinear interaction is supposed to involve more modes excluded from trunction, which will result as a complex external forcing for the reduced model. We model it by adding random noise (in the form of a Gaussian perturbation) to the system. The perturbation is solely applied to the vertical mode $\hat{w}_{01}$, with an amplitude larger than 5% of the mean roll amplitude, then the intermittency can appear in the system as shown in Figure 6.

5 Conclusion

The chaotic behavior of a single convection roll in highly confined, vertical, differentially heated fluid layer is studied. The flow becomes temporally chaotic through a sequence of period-doubling bifurcations.

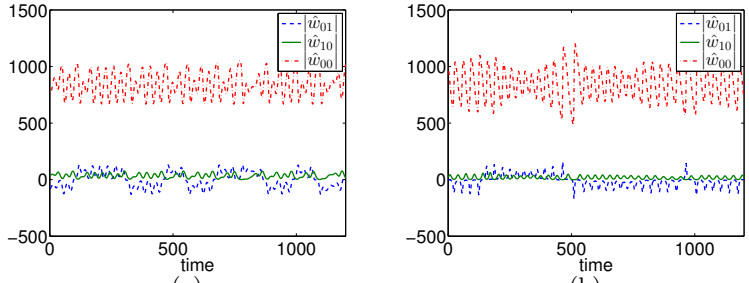

Figure 6. Real part of the Fourier modes $\hat{w}_{01}, \hat{w}_{10}, \hat{w}_{00}$ at $\mathrm{Ra} = 12800$: (a) DNS , (b) model with Gaussian noise of 5% amplitude

A bifurcation diagram is constructed from the temperature timeseries of a point in the flow, which represents some similitude to the one-dimensional map, for example, periodic windows, interior crises. The largest Lyapunov exponent is found to be positive. At higher Ra, a crisis-induced intermittency is observed, whereby the structure makes random excursions between two vertical positions separated by half a wavelength. The mean intermittency period between the excursions scales as $(\mathrm{Ra} - \mathrm{Ra_c})^{0.78}$ over a range of Ra. Two periodic windows corresponding to stable orbits were identified within the intermittent regime. The temporal behavior of the roll can be captured by a three equation model, which are based on the three principal Fourier modes. The model predicts the limit cycles which are close to the ones observed in DNS. By adding a periodic perturbation account for higher-order modes, the model can miminic the chaotic behavior of the roll. Alternatively, intermittency can be obtained by introducing a relatively high amplitude random perturbation to the system. The model displays excursions in phase space corresponding to the roll shift as in DNS. Although the present study was carried out in a domain of small dimensions, we believe that the mechanisms identified here could help us understand the complex dynamics of convection rolls observed in laterally heated cavities.

References

[1] Gao, Z., Sergent, A., Podvin, B., Xin, S., Le Quéré, P. 2013 On the transition to chaos of natural convection between two infinite differentially heated vertical plates *Phys. Rev. E.* **88** 023010

[2] Randrianifahanana. S. 2013 Écoulement de convection naturelle en grande cavité. *Internship report, Master 1, Université Pierre et Marie Curie*

[3] Xin, S., Le Quéré, P. 2002 An extended Chebyshev pseudo-spectral benchmark for the 8:1 differentially heated cavity *Int. J. Num. Meth. in Fluids* **40** 981-998

[4] Feigenbaum, M.J. 1980 Universal behavior in nonlinear systems *Los Alamos Sciences* **1** 4-27

[5] Benettin, G., Galgani, L., Giorgilli, A., Strelcyn, J. 1980 Lyapunov characteristics exponent for smooth dynamical system and for hamiltonian system: a method for computing all of them. *Meccanica* **15** 9-30

[6] Grebogi, C., Ott, E., Romeiras, F., Yorke, J. 1987 Critical exponent for crisis-induced intermittency *Phys. Rev. A* **36** 5365-5380

[7] Melbourne, I., Chossat, P., Golubitsky, M. 1989 Heteroclinic cycles involving periodic solutions in mode interactions with O(2) symmetry. *Proceedings of the Royal Society of Edinburgh: Section A Mathematics* **113** 315–345

[8] Armbruster, D., Guckenheimer, J., Holmes, P. 1987 Heteroclinic cycles and modulated travelling waves in systems with O(2) symmetry. *Physica D* **29** 257–282

[9] Simth, T.R., Moehlis, J., Holmes, P. 2005 Low-dimensional models for turbulent plane couette flow in a minimal flow unit *Journal of Fluid Mechanics* **538** 71–110, 9

[10] Gao, A., Podvin, Z., Sergent, B., Xin, S. 2014 Chaotic dynamics of a convection roll in a highly confined, vertical, differentially heated fluid layer *submitted to Phys. Fluids*